

Understanding the impact of nanostructuring to control neural cell - solid surface interactions at brain-machine interfaces

OTKA NN 116550 – Final report

Motivation

A great deal of research has been performed on central nervous system (CNS) implants to help patients suffering from diseases such as amyotrophic lateral sclerosis, spinal cord injury or paralysis. Effective long-term usage of such devices is limited by the defensive reaction of the CNS resulting in neuronal loss and glial scar formation. These events lead to the signal obstruction between neurons and electrodes during long-term implantation, degrade the performance of the neural electrodes causing instability, and eventually, the failure of the implanted device. The main aims of implant development are to improve neuronal survival and unimpeded regeneration and extension of neurites, while preventing microglial and astrocyte activation by keeping them from attaching to the implanted surface. One of the recent strategies is the topographical modification of neural implant surfaces, as imitating the structure of the extracellular matrix can influence the attachment and behavior of neural cells.

The micro-/nanostructure of the implant surface can have a selective effect on astrocytes and neurons. Proposed explanations by which nanostructuring results in better biocompatibility include the formation of mechanical cues similar to the ECM, and/or the adsorption of growth factors and other molecules facilitating the survival of neurons.

By using micro- and nanomachining techniques, our aim is to develop an implant surface with nanometer-range pattern which could prevent or delay the negative tissue responses to the implanted electrode and thus provides improved neural implants' with long term efficiency. Below is the executive summary of our findings, detailed explanations can be found in the related publications.

Results:

1. Effect of nanostructures on anchoring stem cell-derived neural tissue to artificial surfaces

Different arrangements of nanopatterns were fabricated on silicon wafers (Fig.1.1). These test chips were used to characterize the impact of nanostructuring in attachment, survival and differentiation of neural stem cells and microglial cells on Si and Pt-coated surfaces. The nanostructured surfaces did not exhibit direct toxic characteristics, as neural tissue-like structures developed on each surface (Fig.1.2.-1.3.). The complex cell-assemblies, however, were not anchored on these surfaces: they were washed off easily in form of large floating sheets (Fig.1.4). The detachment indicated strong cell-to-cell interactions without anchor to the artificial surface, and resembled the isolation phenomenon of living tissue from implanted foreign material.

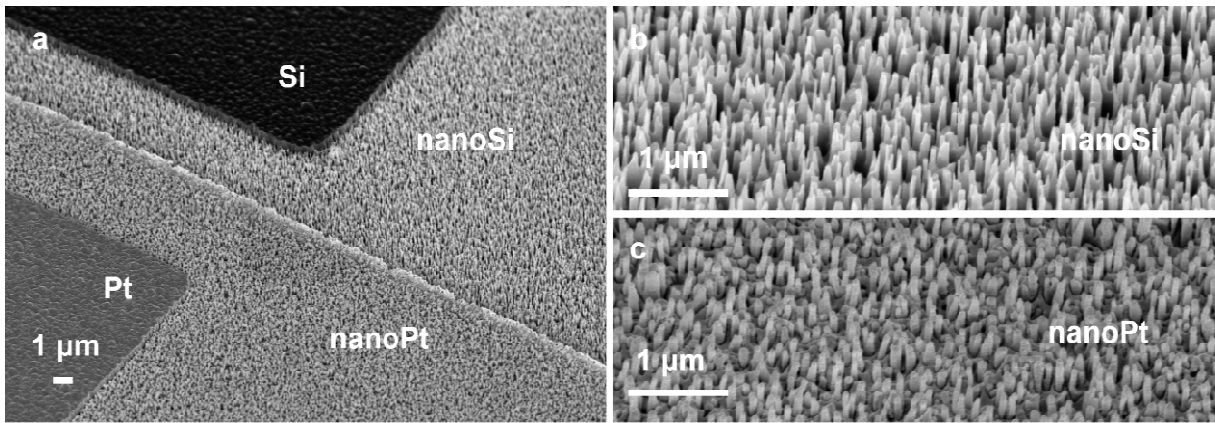
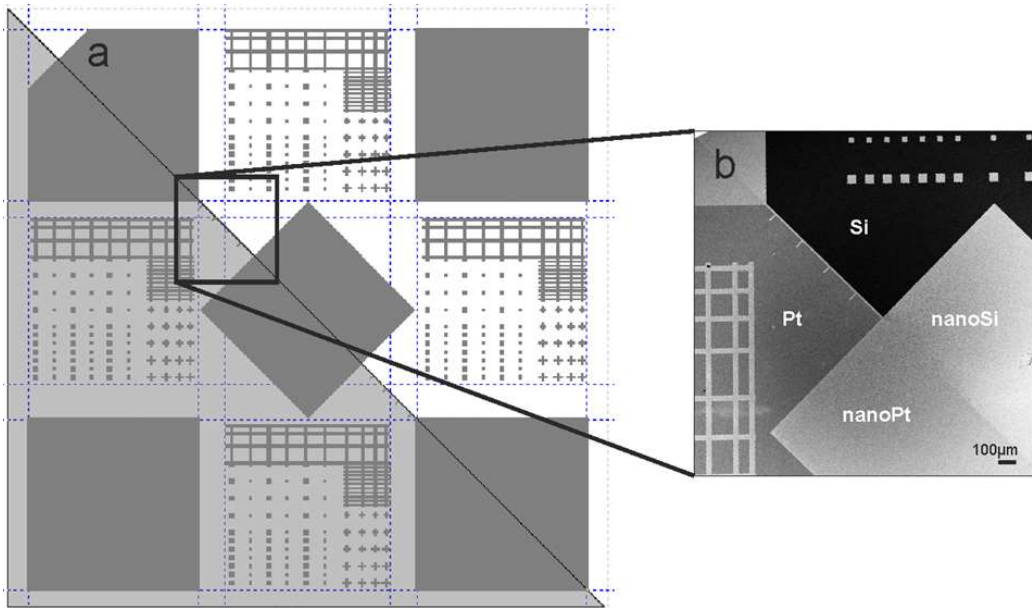
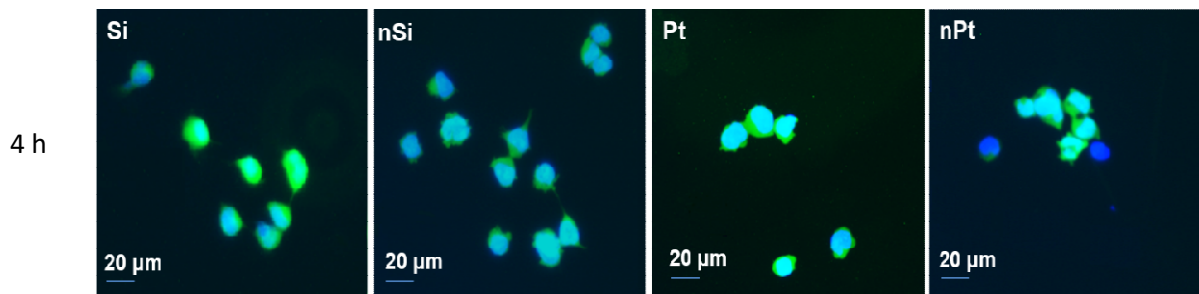


Fig.1.1. a. Schematic view of the 7100×7100 μm² (large) test chip with four different surfaces: Si, nanostructured Si (nanoSi), Pt, nanostructured Pt (nanoPt) including dedicated regions to analyze single cell behavior and statistical behavior of cell populations. b. SEM image of the marked region. SEM micrographs of the four investigated surfaces. a) Part of the chip, where Si and Pt covered plane and nanostructured surfaces are shown. b) 45° tilted SEM image of sharp Si nanopillars made by reactive ion etching of polycrystalline Si thin film c) 45° tilted SEM image of nanostructured Si covered with 30 nm Pt thin film



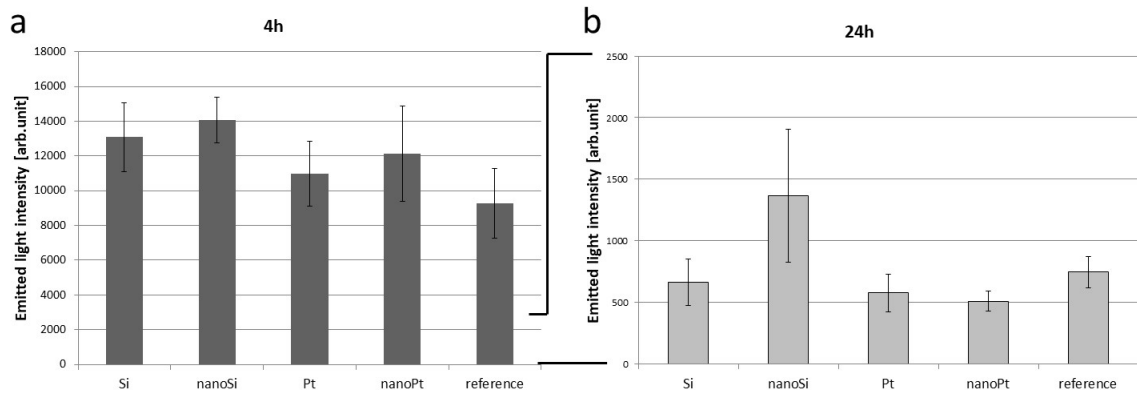
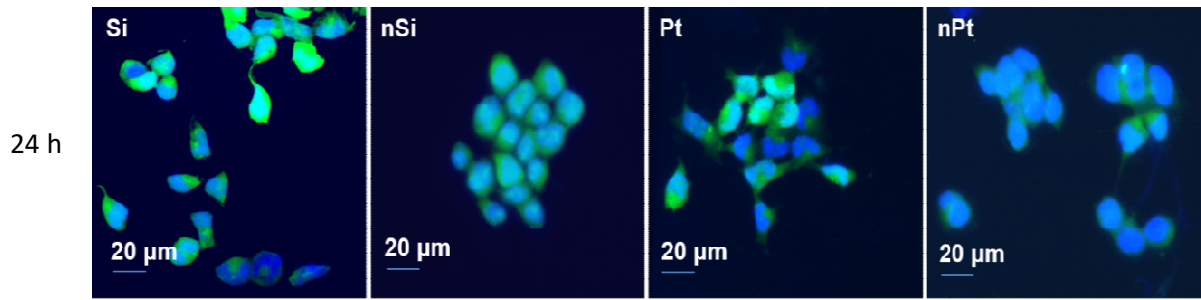


Fig.1.2. Representative fluorescence microscopic images of GFP-NE-4C cells attached to the investigated surfaces after 4 hours and 24 hours. Green: GFP fluorescence, labeling cytoplasm of cells; blue: DAPI fluorescence showing cell nuclei. Nuclear staining-based fluorescence of NE4C cultures after 4-hour (a) and 24-hour (b) cultivation on different surfaces. 4h n: $n_{Si}=8$; $n_{nanoSi}=6$; $n_{Pt}=6$; $n_{nanoPt}=6$; $n_{ref}=6$; 24h n: $n_{Si}=8$; $n_{nanoSi}=4$; $n_{Pt}=6$; $n_{nanoPt}=6$; $n_{ref}=8$

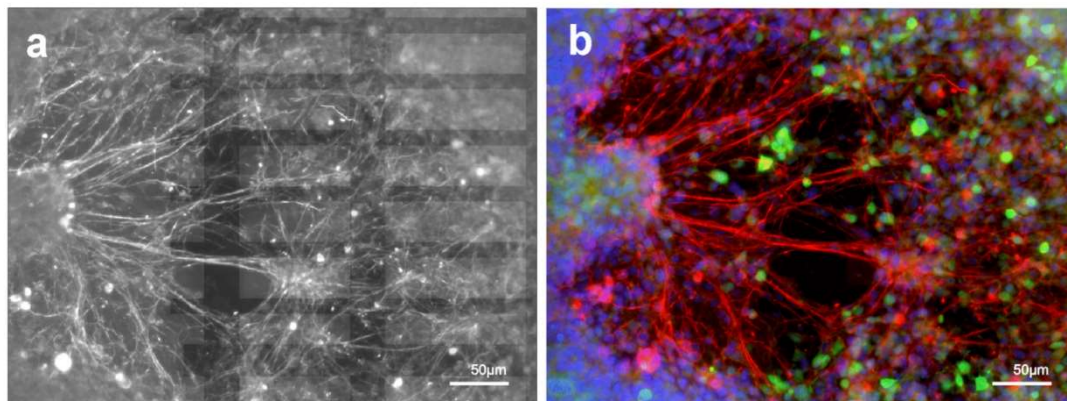


Fig. 1.3. Differentiated neuronal clusters could be fixed mainly on flat silicon surfaces. Neuronal processes, however grew onto nano-structured areas and were visible after fixation and immunocytochemical staining. a: green-fluorescence image showing the surface patterns behind the cells; b: Merged immunocytochemical image of the same field showing III β -tubulin immunoreactive neurons (red) among non-differentiated cells (green: GFP; blue: DAPI).

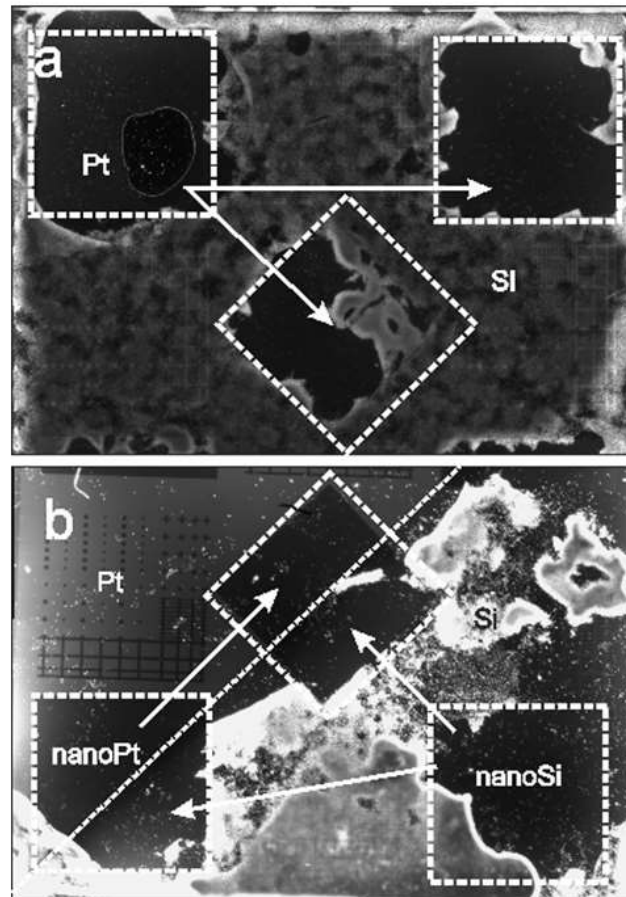


Fig.1.4. Fluorescence images (DAPI channel) of RA-induced GFP-NE-4C cells after fixation. The silicon chips contain poly-Si and Pt surfaces with flat and nanostructured regions. Significantly less or no cells were on the Pt covered regions of the chips, while there is a cell-carpet on the smooth Si side. The cells detached also from the nanostructured Si regions (b).

2. Comparing the effects of uncoated nanostructured surfaces on primary neurons and astrocytes

Commonly used neural implant materials, silicon, and platinum were tested with or without nanoscale surface modifications. No biological coatings were used in order to only examine the effect of the nanostructuring. We seeded primary mouse astrocytes and hippocampal neurons onto four different surfaces: flat polysilicon, nanostructured polysilicon, and platinum-coated versions of these surfaces (Fig.2.1). Fluorescent wide-field, confocal, and scanning electron microscopy were used to characterize the attachment, spreading and proliferation of these cell types. In case of astrocytes, we found that both cell number and average cell spreading was significantly larger on platinum, compared to silicon surfaces, while silicon surfaces impeded glial proliferation (Fig.2.2.). Nanostructuring did not have a significant effect on either parameter in astrocytes but influenced the orientation of actin filaments and glial fibrillary acidic protein fibers. Neuronal soma attachment was impaired on metal surfaces while nanostructuring seemed to influence neuronal growth cone morphology, regardless of surface material (Fig.2.3.). Taken together, the type of metals tested had a profound influence on cellular responses, which was only slightly modified by nanopatterning.

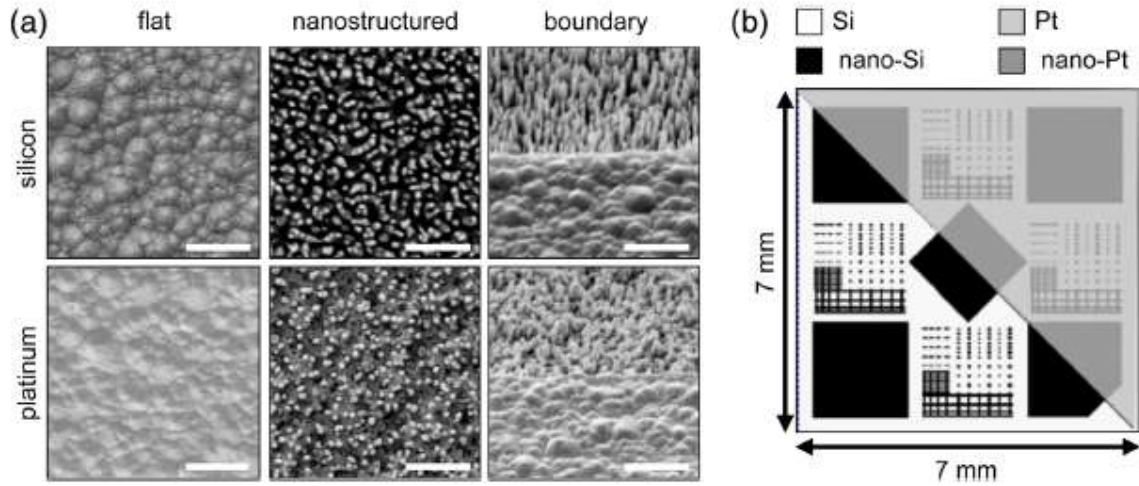


Fig.2.1. Surface and layout of the test chips. (a) Representative images of each experimental surface and the borders between the respective surfaces. Bars denote 1 μm . Left and central panels show surfaces viewed from the top; right panels are shown at a 45.5° angle. (b) Schematic of a single chip used in the study. White surfaces denote flat silicon (Si), black surfaces designate nanostructured silicon (nano-Si). Chips were coated diagonally with platinum, resulting in flat platinum (Pt; light gray) and nanostructured platinum (nano-Pt; dark gray)

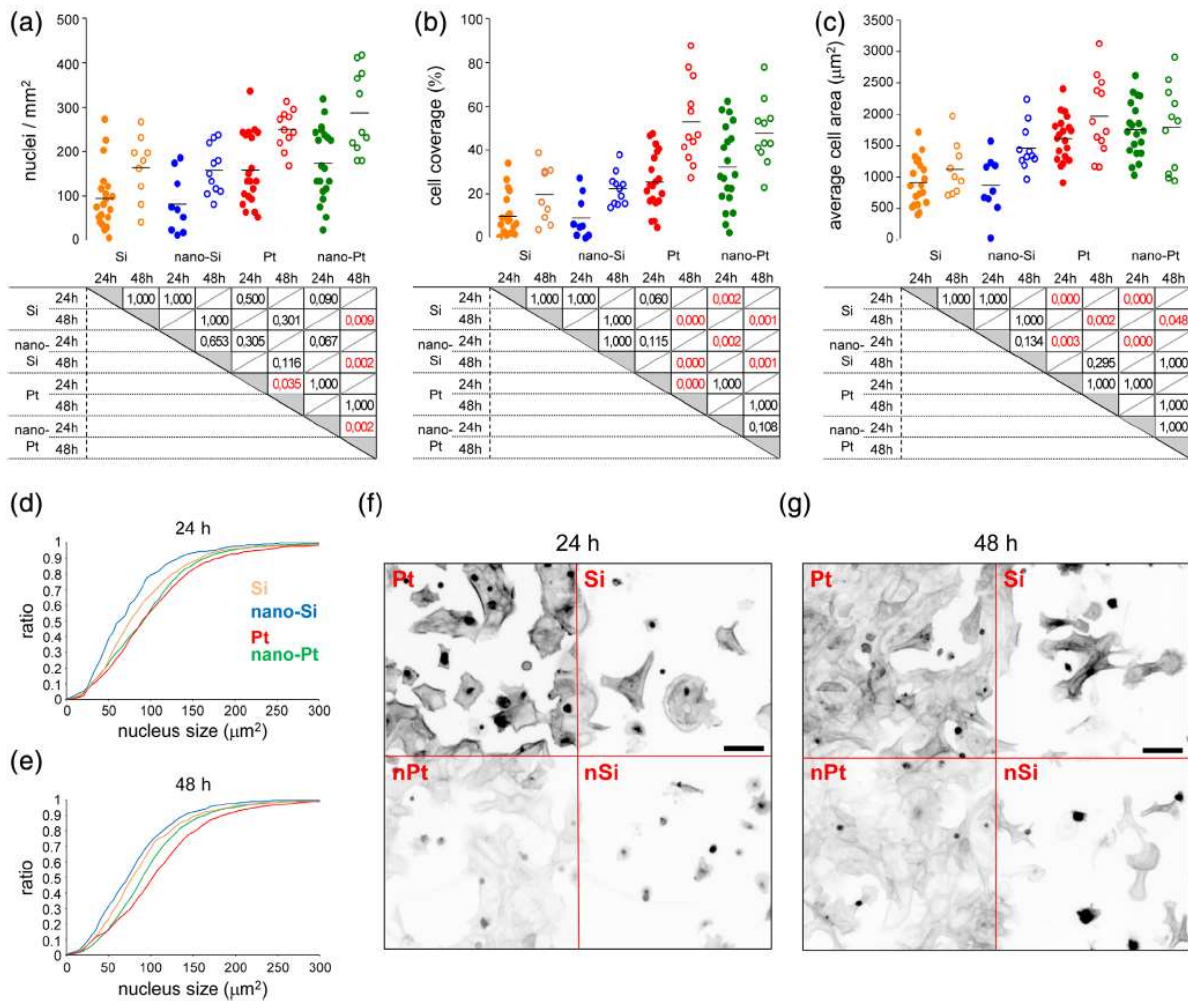


Fig.2.2. Analysis of the total number (a), total surface area (b), average cell area (c) and nucleus size distribution (d-e) of astrocytes on the flat polysilicon [Si], nanostructured polysilicon [nano-Si], flat platinum [Pt] and nanostructured platinum [nano-Pt]. (a-c) Data points show values for the individual ROIs. Horizontal line through data points shows median value. Exact p values are shown in the tables below the graphs, with $p < .05$

in red. (d, e) Cumulative histograms of nucleus size (d) 24 or (e) 48 hr post-seeding. All data were obtained from 3 to 4 independently seeded test chips. Data points per experiment varied between 9 and 20. (f, g) Representative images of primary astrocyte cultures used for quantitative analysis fixed at either (f) 24 or (g) 48 hr post seeding. Inverted images of fluorescent phalloidin staining reveal the actin cytoskeleton of astrocytes over adjacent surfaces. Scale bars denote 100 μm

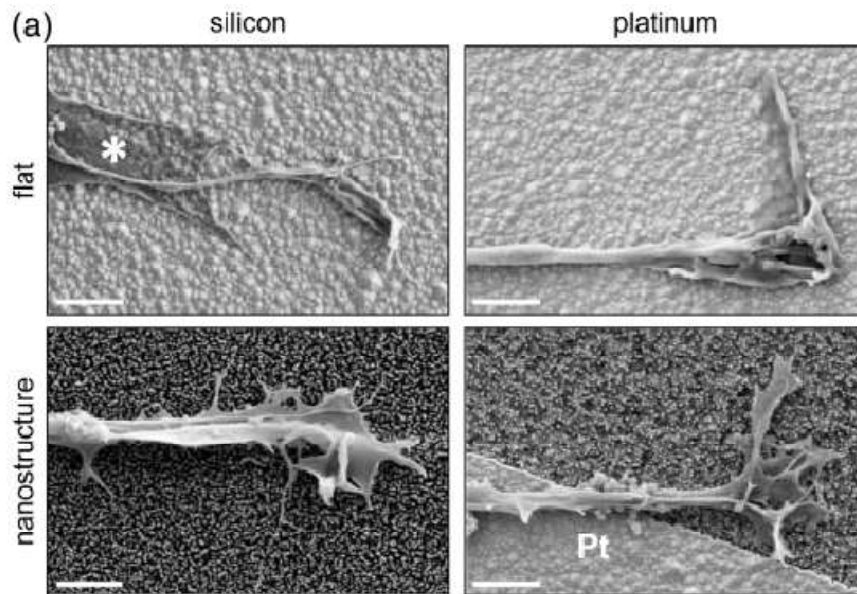


Fig.2.3. Representative images of neuronal growth cones directly attached to the different uncoated experimental surfaces. Representative images produced by scanning electron microscopy. Asterisk in the upper left image marks the edge of a glial process. Scale bars denote 2 μm .

3. *In vivo* neurobiochemical changes in the vicinity of a nanostructured neural implant

We investigated the chronic effect of four different surface topographies on the brain tissue *in vivo*. The four different surfaces are the following: (1) polycrystalline Si with 100–200 nm grain size, and with a surface roughness factor of 1.04 (calculated as the ratio of the measured and the projected surface area of AFM images) therefore considered to be the flat reference; (2) the backside of the non-polished Si wafer with a polySi layer with around 2 μm surface patterns; (3) 1–2 μm ridges covered by fluorocarbon polymer; (4) nanostructured surface with a pillar height of 580–800 nm and with a pillar density of 18–70 pillars/ μm^2 .

Cross sectional view of the process flow of test probes with different surfaces are shown on Fig. 3.1. After 8 weeks of implantation time, brain tissue sections were stained with NeuN and GFAP to visualize viable neurons and gliosis, respectively. Optical microscopic images were evaluated using quantitative image analysis. Significantly more neurons were present adjacent to the nanostructured surfaces compared to all the others in the first 50 μm . Less severe gliosis could be observed around the nanostructured surface from 50 μm up to 300 μm compared to the others, but this difference was not significant. A massive glial scar was visualized around all types of the investigated surfaces in the first 50 μm .

Our results suggest that surface topography can alter the effect of implantation regarding the preservation of neurons in a distance of 0–50 μm from the track (Fig.3.2.). Nanostructuring the implant surface may be favorable for long-term applications as a larger neuronal density remains in the vicinity of a nanostructured surface and may provide better signal-to-noise ratio during electric recordings.

Although it is clear that radical changes can be reached by surface adhesive protein coatings, it is still a question how long that solution can work. It will be important to complete these findings with the

implantation of functional electrodes and recordings over long time periods to observe the practical effects of surface modifications to the long term stability of CNS implants.

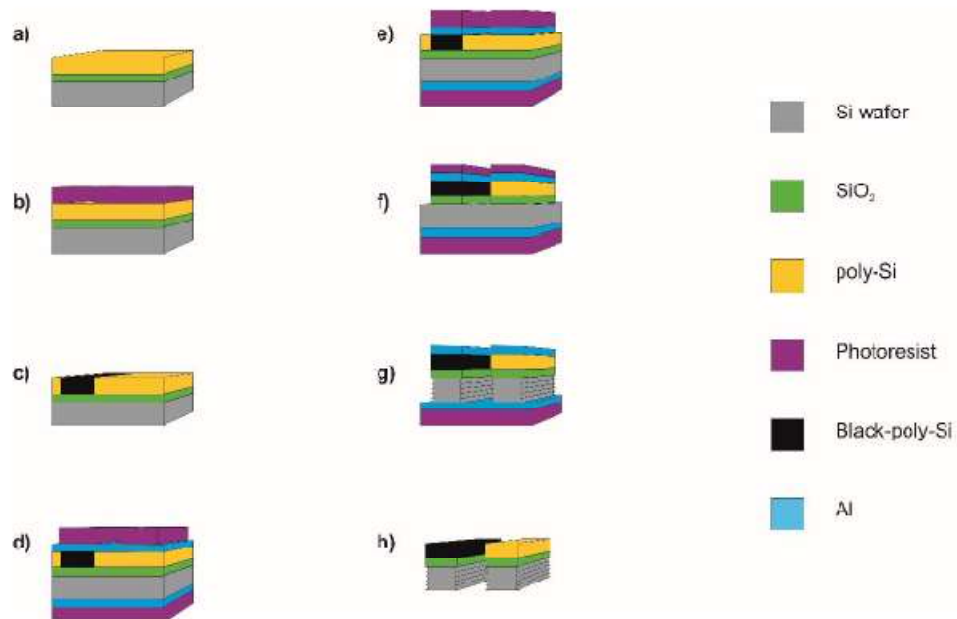


Fig. 3.1. Schematic cross sectional view of the microfabrication process of the probes. The fabrication steps are the following: a) thermal SiO₂ growth (500 nm) and polycrystalline Si (1000 nm) deposition, b) photolithography: masking of the nanostructured parts, c) black Si formation by deep reactive ion etching d) deposition of an Al masking layer (300nm) and photoresist for device contour definition e) photolithography, Al etching, f) PolySi and SiO₂ dry etching, g) through-wafer etch of silicon by Bosch recipe, h) photoresist and Al removal from the front- and backside.

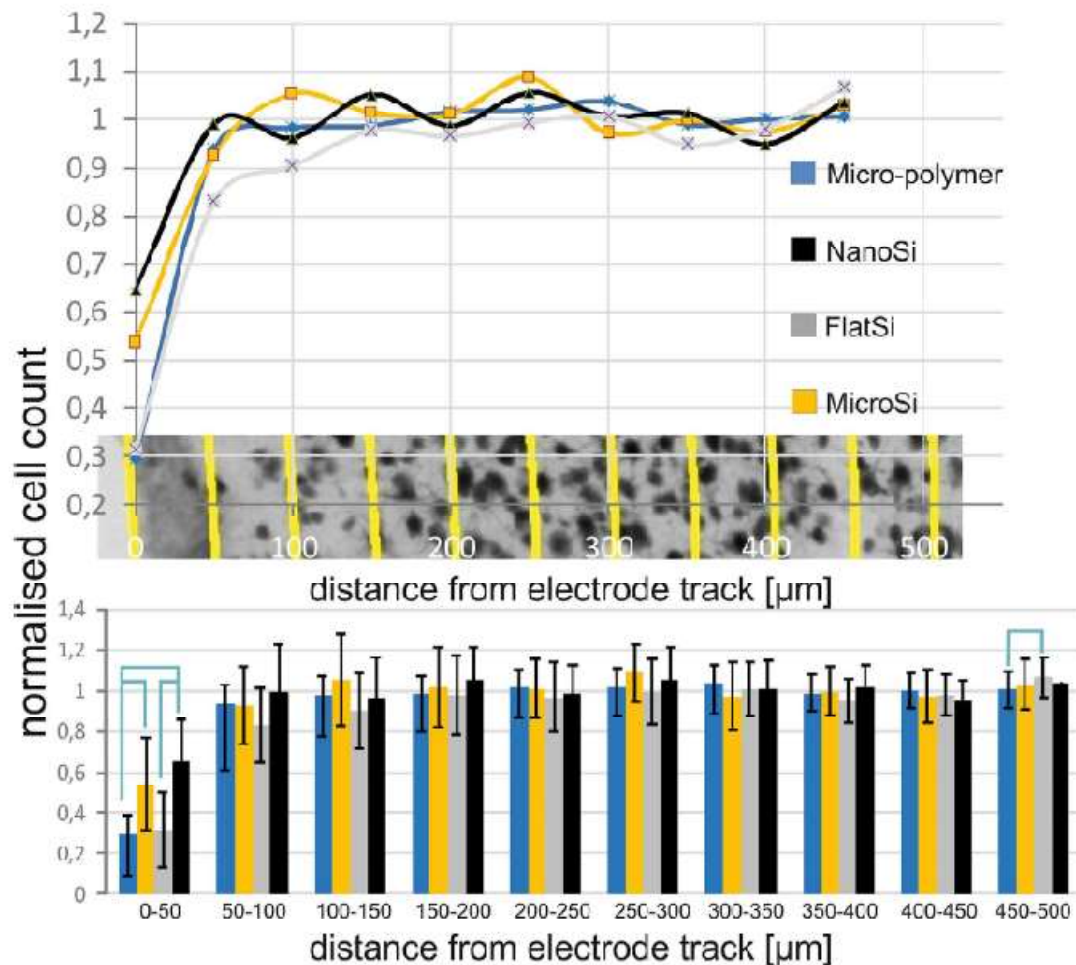


Fig.3.2. Results of the neural cell count quantification. Increasing neural density can be measured with the distance from the electrode track. After the first 200 μm there was no considerable change in neural cell number in function of the distance. In the first 50 μm , which is considered as the recording distance of a microelectrode, a significant difference was found in average neural cell density in case of surface properties. The highest neural cell loss was found at the microstructured fluorocarbon polymer covered surface, while the highest neural cell density appeared at the proximity of nanostructured implant surfaces. Significant difference was found between the flat and nanostructured Si surfaces implying that nanotopography is favoured by neurons within the distance relevant in neural recording. ($N_{\text{Micro-polymer}} = 50$, $N_{\text{MicroSi}} = 25$, $N_{\text{FlatSi}} = 23$, $N_{\text{NanoSi}} = 23$) Sample means and standard deviations are presented.

4. 3D arrays of microcages by two-photon lithography for spatial organization of living cells

A new approach to enable formation of artificial 3D cell networks using two-photon lithography was demonstrated by IMTEK with the close collaboration of Dr Zoltán FEKETE in sample fabrication and publication. The concept is based on stacking layers of cell-sized, container-shaped microcages designed for hosting cell cultures (Fig. 4.1). The hemispherical microcages were optimized to host most likely a single cell and to keep it in place, while allowing it to extend neurites to cells in neighboring cages. The structures comprise features allowing them to be stacked layer by layer, thus forming an arrangement of microcages with the periodicity of a facecentered cubic lattice. Biocompatibility of the structures was proved by observing the viability of cells cultured on them. Neuron-like PC12 cells grow on and within such stacked microscaffolds and outgrow neurites through cage boundaries as a first step towards controlled 3D cell networks.

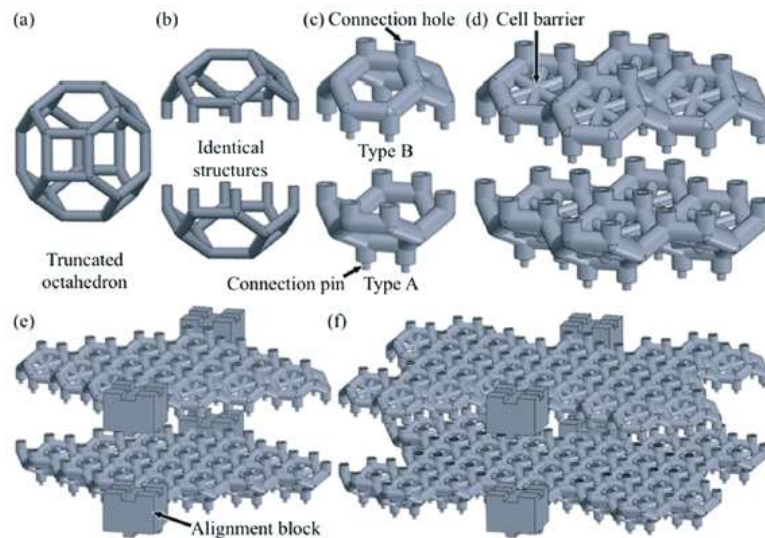


Fig. 4.1. Concept of microcages for the 3D controlled cellular network (a) inspired by the geometry of a truncated octahedron (b) cut into two identical structures. (c) Both structures were created to be robust by thickening their edges; connection holes and pins were added to create type A and type B structures. (d) Initial structures are reproduced periodically in 2D and cell barriers are added to obtain 2×2 unit structures. (e and f) Larger structures used in the experiments are built from these unit structures, with cuboid blocks added to their sides for manipulation and alignment.

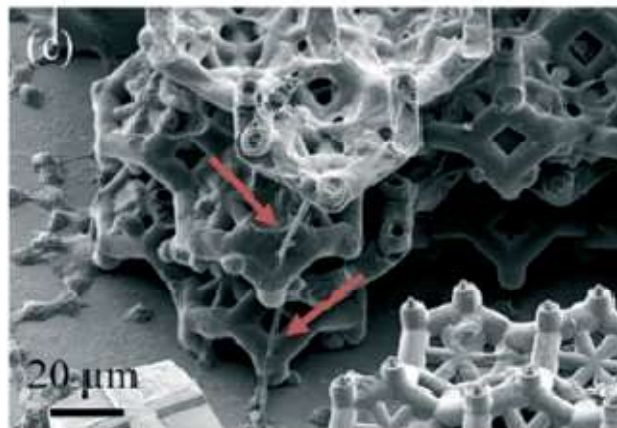


Fig.4.2. SEM micrographs of a tri-layer stack of structures with cells, neurites bridging layers and thereby creating 3D neuronal networks (denoted by red arrows).

5. Modification of glial attachment by surface nanostructuring of SU-8 thin films

To create our surface patterns, we used the biocompatible, epoxy-based negative photoresist, SU-8. SU-8 structures were patterned by standard photolithography and electron beam lithography depending on the desired feature size. The optimal irradiation depends on the sensitivity of the photoresist type, its thickness and the electron energy. These parameters were investigated preliminarily to form nanostructures with the desired geometry. To produce structures at the sub-micron scale, O₂ plasma etching was used. Representative features are shown in Figure 5.1.

In vitro test chips were designed to investigate the cell-nanostructure interaction on different SU-8 surfaces using fluorescent microscopy and scanning electron microscopy. We found that shape and density of SU-8 nanostructures strongly affect the attachment of primary mouse astrocytes, opening up the way to control glial attachment by local nanoscale surface modification of polymer thin films. Representative results are shown in Figure 5.2.

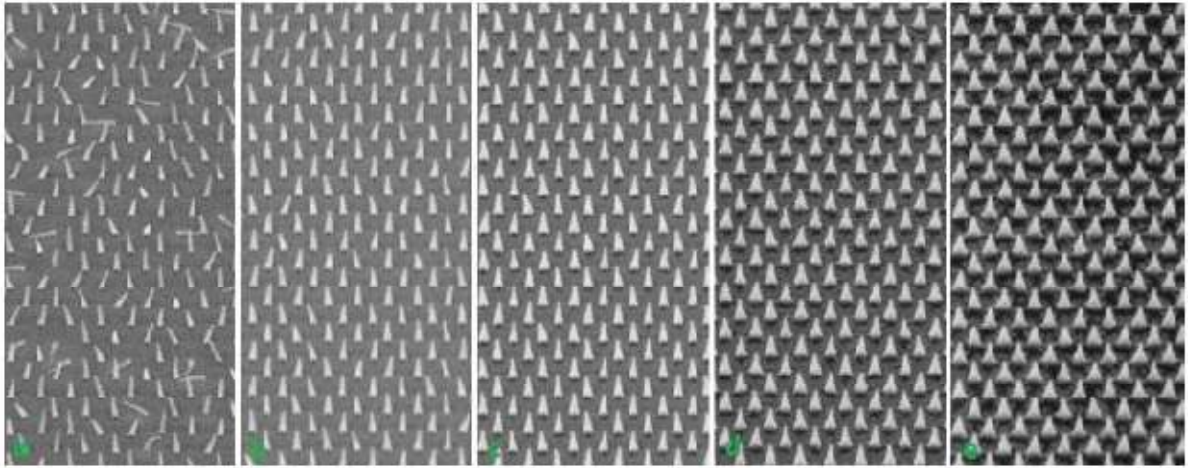
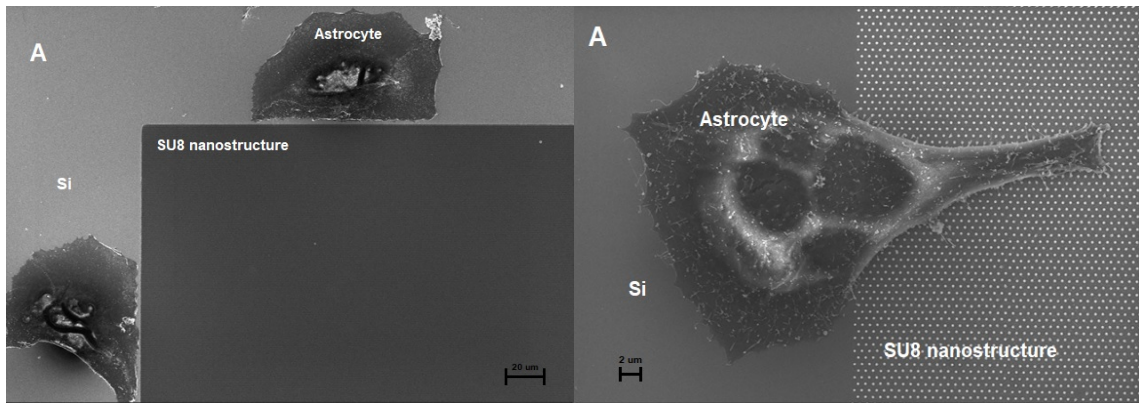
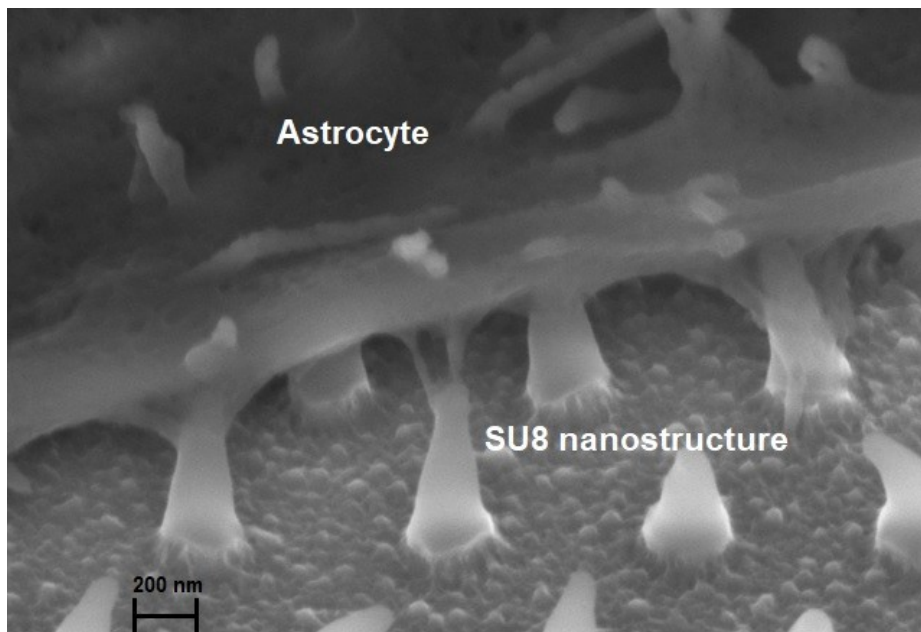


Figure 5.1. SU-8 nanostructures fabricated using different e-beam lithography parameters. The center-to-center distances are 500 nm.



(a)

(b)



(c)

Figure 5.2. Primary mouse astrocytes avoid type A nanostructured SU-8 surfaces (a), while spread over type B nanostructured surfaces (b) and attach to spiky SU-8 nanopillars (c).

Conclusion and outlook

Based on our findings on nanostructured surfaces neuroectodermal stem cells are able to differentiate into neurons under appropriate conditions, and the formed neurons develop basic networks. In contrast, the developed „tissue model” cannot be kept on platinum surfaces as the adhesion between cells is much stronger than between cells and the artificial surface. The platinum preference of BV2 microglial and primer astroglial cells also suggest that platinum is not the best surface in terms of long-term biocompatibility. From *in vivo* measurements, we concluded that more viable neurons can be counted adjacent to the nanostructured Si surface compared to flat or microstructured Si surfaces, which implies that the nanostructuring of the implant surface may be beneficial. Platinum is a commonly used material for neural implants, as it is non-toxic, and has relatively low impedance at frequencies relevant in brain signal recording. The increase of the specific surface area due to nanostructuring may partly compensate the above described negative effects. It should be noted that on the implant surface most used, only the recording sites are covered by platinum, and the rest of the surfaces are composed of either silicon or dielectric materials, which cover significantly larger areas. Nanostructuring these areas by the described method may promote neural cell viability near the implant.

Cell culturing on micro and nanostructured polymer surfaces opens up a new world for neural implant development. We demonstrated that the shape and density of SU8 nanostructures influence the attachment of glial cells, so that glial repellent surfaces can be created. The combination of nanostructuring techniques with emerging polymer materials – e.g. shape memory polymers – are a promising developmental paths for novel, long-term neural implants.

Indicators:

Number of PhD theses: 4 (finished and on-going)

Number of MSc, BSc theses, TDK: 6

Number of Q1 articles: 7 (D1: 5)

Cumulative impact factor of the articles: 35.016

List of publications

Bérces et al, Neurobiochemical changes in the vicinity of a nanostructured neural implant, Scientific Reports6 (2016) 35944, doi: 10.1038/srep35944, IF: 4.259

H. Liliom et al: Differential effects of nanostructuring on primary neurons and astrocytes, Journal of Biomedical Materials Research: Part A (2019), in press, doi: 10.1002/jbm.a.36743, IF: 3.221

Bérces et al, Effect of nanostructures on anchoring stem cell-derived neural tissue to artificial surfaces, Journal of Neural Engineering 15 (2018) 056030, doi: 10.1088/1741-2552/aad972,IF: 4.551

Z. Fekete, A. Pongracz: Multifunctional soft implants to monitor and control neural activity in the central and peripheral nervous system: A review, Sensors and Actuators B 243 (2017) 1214-1223, doi: 10.1016/j.snb.2016.12.096, IF: 5.667

F. Larramendy et al 3D arrays of microcages by two-photon lithography for spatial organization of living cells, Lab on a chip 19(2019) 875-884, doi: 10.1039/C8LC01240G, IF: 6.914

A. Zátonyi et al A softening laminar electrode for recording single unit activity from the rat hippocampus, Scientific Report 9 (2019) 37237, doi: 10.1038/s41598-019-39835-6, IF: 4.011

D. Meszéna et al A novel, silicon-based spiky probe providing improved cell accessibility for in vitro brain slice recordings, *Sensors and Actuators B* 297 (2019) 126649, doi: 10.1016/j.snb.2019.126649, IF: 6.393

A. Pongrácz et al Modification of glial attachment by surface nanostructuring of SU-8 thin films, *MDPI Proceedings* 2(2018) 1016, doi: 10.3390/proceedings2131016